Time and Frequency Domain CCD-Based Thermoreflectance Techniques for High-Resolution Transient Thermal Imaging

B. Vermeersch[1,2], J. Christofferson[1], K. Maize[1], A. Shakouri[1], G. De Mey[2]
[1] Jack Baskin School of Engineering, University of California, Santa Cruz CA 95064
[2] Dept. of Electronics and Information Systems, Ghent University, Belgium

Abstract

Thermoreflectance microscopy is a well established method for the thermal imaging of (opto)electronic components and ICs. The technique combines submicron spatial resolution with excellent temperature resolution (10 mK can be achieved). The dynamic thermal behavior can be studied using either a transient pulsed boxcar or frequency domain approach, the latter including homodyne and heterodyne lock-in systems. Temporal scales in the nanosecond range can be resolved. The basic principles of the various methods are reviewed, and their associated advantages and drawbacks are compared. We also propose a novel heterodyne technique as an alternative to the 'four bucket' method that has been used so far. Our approach greatly reduces the timing complexity while eliminating a major source of systematic error. Illustrative case studies present the transient and AC heat diffusion in integrated gold heaters, and separate imaging of Joule and Peltier effects in a $20 \times 20\,\mu\text{m}^2$ thermoelectric microcooler.

Keywords

Thermoreflectance, imaging, transient, pulsed boxcar, homodyne, heterodyne, ultra-fast, high-resolution, CCD

1. Introduction

Thermoreflectance imaging offers an interesting tool for accurate, non-contacting thermal characterisation of electronic devices. An extensive review on the general principles and wide range of applications of the technique can be found in [1].

Essentially the method relies on the small but detectable variation of the optical reflectivity of the device under test (DUT) with temperature. This dependence can be linearised around a reference (ambient) temperature, as quantified by the thermoreflectance coefficient C_{TR}. This parameter expresses the relative change in reflectivity per degree of temperature deviation from ambient:

$$C_{TR} = \frac{1}{\Delta T}\frac{\Delta R}{R} \quad \Rightarrow \quad \Delta T = \frac{\Delta R}{C_{TR} \cdot R} \tag{1}$$

Typically C_{TR} is in the order of 10^{-4}/K. A blue or green light emitting diode (LED) uniformly illuminates the DUT under a microscope, while a charge coupled device (CCD) camera captures the reflected light. From the difference between the 'hot' image (DUT active) and 'cold' image (DUT in off state) the temperature distribution can be determined using (1), provided that adequate in-situ C_{TR} calibration is performed.

Since visible optical wavelengths are used, the achievable spatial resolution is at least one order of magnitude better than the one obtained with traditional infrared thermography. The temperature resolution, on the other hand, seems limited by the small C_{TR} values combined with the mapping of the reflected signal to the discrete grey levels in every pixel of the CCD. However, noise usually causes the signal to fluctuate over several levels. Through averaging over a sufficient number of exposures, the effective temperature resolution can be largely enhanced [2]. This phenomenon, known as stochastic resonance, is able to extend the dynamic range of a 12-bit CCD to over 18 effective bits, allowing measurements with temperature resolutions of 10 mK [2].

Although steady state images can already reveal a lot about the device heating, it is in many applications desirable to observe how the heat diffusion evolves dynamically. Systems able to visualise these temperature transitions have been developed. Both transient (time domain) or frequency domain (AC) thermoreflective imaging techniques can be used to acquire the dynamic thermal behavior. Each variant is discussed in the rest of the paper and illustrated by means of experimental case studies.

2. Time Domain Techniques

Transient schemes make it possible to directly see the time evolution of the thermal signal. Due to the small size of electronic components, the relevant transients may occur over time scales of microseconds and shorter. Even with ultra-fast (≈500 fps) CCD cameras these transitions are much too quick to track real-time. Instead, we have developed a different method to capture the thermal transients [3, 4].

2.1 Pulsed boxcar averaging

In order to obtain thermal images at a higher temporal resolution than the frame rate of the CCD, a short duration LED pulse is used to strobe the temperature at different times. LED's are easily pulsed to 100 nanoseconds, and a pulsed laser can be used to image in the picosecond regime. Carefully adjusting the timing delay relationship between the short LED pulse and the signal applied to the DUT allows for a thermal image 'snapshot' corresponding to a programmed delay in the temperature cycle.

To obtain reasonable signal-to-noise ratio (SNR) in the thermal image, the total illumination reflected off the sample and recorded in the CCD must exceed a minimum intensity. This minimum required intensity is much greater than the amount of light that can be reflected during a single short pulse. To ensure a reasonable SNR in the thermal image, many heating and measurement periods occur for each CCD frame. Typically the LED is run at a 1% duty cycle, and the device at 25%. Device excitation is always kept below 50% duty cycle to ensure that the device cools back to room temperature before the next heating cycle.

Time domain thermoreflectance thermal imaging creates a differential temperature map, meaning that the thermal images represent the value of the device's temperature compared to the unexcited device. Therefore, we are always comparing the value of the CCD signal before the device is excited (delay 0), to the temperature at a preprogrammed delay. To accomplish this the free-running timing signals are gated, such that the system rapidly switches from delay 0 to a pre-programmed delay set by the user between every CCD frame. The thermoreflectance signal is thus obtained at the half frame rate of the CCD, and thus acts as a noise rejecting frequency domain filter. The computer then can sweep through many delays to obtain a thermal imaging movie of the active device. Details of the timing and the system have been presented previously [4].

One advantage to this method is that the thermal images can be obtained with time scales from 100 ns to 10 ms representing about 5 orders of magnitude in time. This allows for thermal imaging of different effects at different timescales. In order to see thermal device behavior over many orders of time, it is possible to perform a logarithmic time sweep. Using this technique we obtain the thermal step response of the device.

2.2 Case study: gold heater on silicon substrate

Figure 1 shows short and long time scale thermal imaging of a 100 micron integrated gold heater using pulsed boxcar averaging. As expected, we can observe rapid heat diffusion in the device metal, owing to the heater's small thermal mass and thermal conduction by free electrons. This is then followed by a slower diffusion in the semiconductor substrate. The circular 'halo' around the heater, vaguely appearing from 60 μs and clearly visible by 3 ms, indicates radial heat spreading in the substrate.

2.3 Case study: ultrafast characterization of microcoolers

Figure 2 shows the step response of two different superlattice micro-cooler devices of different sizes and currents, as compared to a micro-cooler with no superlattice. The devices are excited by a current step, larger than for optimum cooling, but even at large currents the superlattice devices momentarily cool for several tens of microseconds before the slower Joule heating leads to an overall net heating. The results are carefully studied, and modeled to increase the understanding of cooling perfomance of superlattice devices.

3. Frequency Domain (AC) Techniques

Frequency domain methods consist of analysing periodic temperature oscillations, induced by a sinusoidal excitation of the DUT. These measurements, too, reveal a lot about the dynamic thermal behavior of the IC under study, although the information is contained in a more abstract form and less directly accesible as compared to time domain counterparts. Still, both approaches are in principle entirely equivalent, and mathematically related through Fourier transforms. Intuitively, one can expect a connection between the magnitude of the temperature oscillation at a frequency f and the transient temperature observed in the heating curve at time $t = \frac{1}{\omega} = \frac{1}{2\pi f}$. A relatively firm relation can indeed be derived based on underlying physical and mathematical principles [5]. The function generators currently at our disposal enable frequencies up to 30.2 MHz, yielding an equivalent time resolution of approximately 5 ns.

AC techniques involve a lock-in mechanism: precise timing provokes the setup to be 'tuned into' a specific frequency, thereby rejecting other signals. Consequently, these methods are known to be more robust to noise than transient techniques [6]. In addition, they provide on-the-fly phase images, which have proven to be quick and sensitive heating detectors. Spots where very weak heating occurs can be identified with far less averaging than would be required to resolve the spot in the magnitude signal. Finally, AC measurements enable separation of Joule and Peltier effects, which is particularly useful for the analysis of thermionic and thermoelectric microrefrigerators (see further in section).

Two variants of AC techniques can be distinguished, as discussed below.

3.1 Homodyne methods

Homodyne setups supply a sinusoidal signal to the DUT while continuous-wave illumination is used, i.e. the optical pulse repetition frequency is zero. The signal being reflected to the detector can be written as:

$$s(x,y,t) = R_0(x,y) + R_1 \cos(2\pi f t + \varphi(x,y) + \varphi_S) \qquad (2)$$

in which R_0 and R_1 are the DC and AC magnitude respectively, $\varphi(x,y)$ the phase shift induced by thermal inertia of the DUT, and φ_S represents any potential phase shift introduced by the setup. The CCD frame rate is set to precisely $4f$ in order to oversample the signal by a factor 4. That way, the consecutive camera exposures correspond to quarter-period integrals of the signal:

$$I_n = \int_{(n-1)T_s/4}^{nT_s/4} s(x,y,t)\mathrm{d}t \quad , \quad n = 1 \cdots 4 \qquad \text{with} \quad T_s = \frac{1}{f} \quad (3)$$

One can prove [7] that the magnitude and relative phase information can then be extracted as:

$$\begin{aligned} R_0(x,y) &= \frac{1}{T_s}(I_1 + I_2 + I_3 + I_4) \\ R_1(x,y) &= \frac{\pi}{\sqrt{2}T_s}\sqrt{(I_1 - I_3)^2 + (I_2 - I_4)^2} \\ \varphi(x,y) + \varphi_S &= -\arctan\left(\frac{I_1 + I_2 - I_3 - I_4}{I_1 - I_2 - I_3 + I_4}\right) \end{aligned} \qquad (4)$$

The implementation of a homodyne system is relatively simple, although this comes at the cost of a bandwidth limited by the camera frame rate, since ultimately the method requires a real-time tracking of the oscillating temperature field. Typically, $f_{\max}$ is a few tens of Hz at best, rendering the technique only suitable for quasi-steady state experiments. Still, the homodyne approach is highly preferable to direct DC measurements, because the lock-in mechanism encompassed in the former provides a robust rejection of noise and spurious signals with frequencies not equal to f.

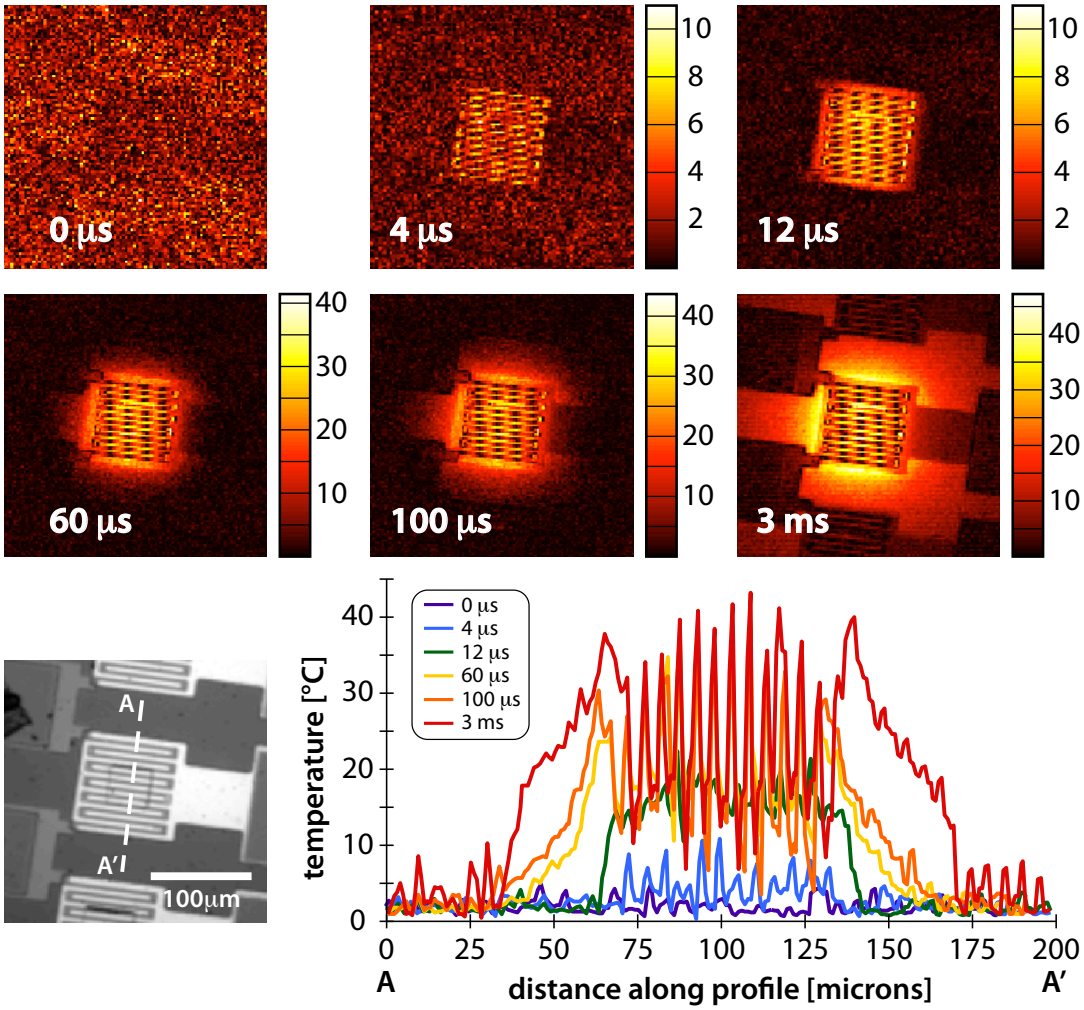

Figure 1: Time domain thermoreflectance imaging of a 100 micron heater using 'pulsed boxcar averaging'. Thermal images present ΔT in °C.

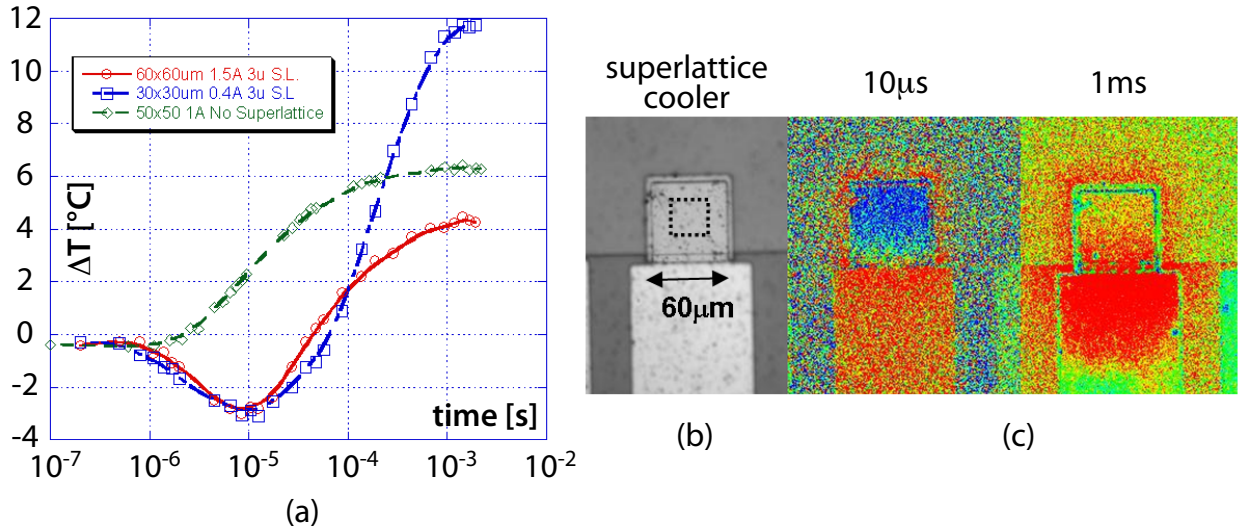

Figure 2: Transient thermal imaging of microcoolers: (a) step response of 3 different devices; (b) investigated superlattice cooler with indicated surface temperature assessment region; (c) thermal images at different points in thermal cycle.

3.2 Heterodyne methods

Put in simple words, a heterodyne setup operates as an advanced stroboscope. The method employs sinusoidal/pulsed signals on both the DUT excitation and LED illumination sides. This induces natural mixing in the optical domain. The left sideband of the reflected signal, at the frequency difference between the oscillating DUT temperature and LED pulses, is a slowly blinking pattern that can be captured by the CCD camera. The technique greatly extends the limited bandwidth attainable by homodyne methods to several tens of MHz. Obviously, however, additional strict timing requirements come into play.

Established approach: '4-bucket'

Heterodyne thermoreflectance experiments published in literature so far have all adopted a method developed by Grauby and his co-workers [7]. In order to capture temperature oscillations at frequency $2F$, pulsed illumination is used, with frequency $2F+f$. The reflected signal hence contains a slowly blinking term at frequency f. This image is sampled by the CCD running at frame rate $4f$ and processed in exactly the same way as for the homodyne case. It has been demonstrated [2] that with this heterodyne technique a temperature resolution about 10 mK can be achieved, with a spatial resolution down to 250 nm when blue light is used. It should, however, be noted that achieving such supreme temperature resolutions come at the cost of extremely long averaging times in the order of 10 hours or more, which may be unsuitable for practical purposes.

Grauby's method is sometimes denoted as the 'four bucket' technique, a name referring to the 4 image containers I_n corresponding to the quarter-period integrals (3) of the reflected signal. However, this may prove to be a weak point in the approach. Namely, an actual system will not be able to entirely fill the buckets, since a certain amount of time is required to read out the CCD sensor and transfer the data to an external processing unit. The camera we use in our experiments (1.36 Mpixels, frame rate ≤ 20 fps) could achieve a maximum duty cycle of about 90%, meaning that 10% of each integral is overlooked. Further analysis shows that this dead time, depending on its position with respect to the signal maximum, induces amplitude underestimations between 8 and 11% and phase deviations between -4.5 and 4.5 degrees. Since the relative position of the dead time intervals is not known a priori and will vary randomly between experiments, these systematic errors cannot be corrected for.

Novel approach: 'cycled phase lag'

In order to overcome this problem, we have developed a novel heterodyne method. Full details on the technique will be presented elsewhere [8]. The main idea is to use an LED pulse frequency of $2F$, i.e. simply equal to that of the thermal field under study. The blinking term reduces to a static image of the form

$$J_1 = R_0(x,y) + \xi \cdot R_1(x,y)\cos\left(\varphi(x,y)+\varphi_S\right) \qquad (5)$$

with ξ a form factor parameter of the optical waveform (e.g. $\xi = \frac{2}{\pi}$ for square pulses). Since no time dependence is left in (5), the signal integration performed during CCD exposure is nothing else than a scaling. The frame rate and other settings of the CCD can be chosen arbitrarily, offering opportunities to optimise the optical quality and dynamic range of the image. The allowance for a free-wheeling camera also brings the strict timing requirements down to a simple phase-locking of two function generators.

However, in the image J_1 the DC term, AC magnitude and phase are all intermingled. A solution is provided by deliberately introducing a phase delay Ψ (relative to the illumination pulses) into the DUT excitation signal. Cyclic alteration of the phase lag can be easily automated by adjusting the initial waveform phase of the corresponding function generator. Using well chosen phase increments (45/90 degrees for Joule/Peltier effects respectively) provides the following additional images:

$$\begin{aligned} J_2 &= R_0(x,y) + \xi \cdot R_1(x,y)\sin\left(\varphi(x,y)+\varphi_S\right) \\ J_3 &= R_0(x,y) - \xi \cdot R_1(x,y)\cos\left(\varphi(x,y)+\varphi_S\right) \end{aligned} \qquad (6)$$

The desired AC magnitude and relative phase can now be recovered as

$$\begin{aligned} R_1(x,y) &= \frac{1}{\xi}\sqrt{\left(\frac{J_1-J_3}{2}\right)^2+\left(\frac{2J_2-J_1-J_3}{2}\right)^2} \\ \varphi(x,y)+\varphi_S &= \arctan\left[\frac{2J_2-J_1-J_3}{J_1-J_3}\right] \end{aligned} \qquad (7)$$

We have used our novel 'cycled phase lag' technique for heterodyne thermal imaging for two case studies presented below. Table 1 summarises all AC techniques just discussed by listing the frequencies involved, typical bandwidth and complexity of the various methods.

3.3 Case study: gold heater on silicon substrate

We have investigated a 40 micron heater. Thermal magnitude and phase images at various frequencies are presented in Fig. 3. The behavior is very similar to the one observed with time domain imaging. At large frequencies (corresponding to short time scales) heating is localised to the device itself, and then later (at lower frequencies) followed by thermal diffusion in the silicon. Once again radial heat spreading in the substrate can be concluded based on the circular halos, which are clearly visible in the phase as well. The connection between AC and transient modes can also be understood in terms of the thermal penetration length $l = \sqrt{\frac{2D}{\omega}} = \frac{D}{\pi f}$, with D the thermal diffusivity. Using silicon parameters and setting l to the heater size of 40 microns leads to $f \approx 20$ kHz. We see that substrate heating indeed becomes visible in the measurements for $f \leq 10$ kHz. We have checked that numerical AC simulation of a simple device model leads to images very similar to the experimental ones, for both magnitude and phase. Finally, we note that the anomalously large increment of the relative phase at 500 kHz is caused by a sudden increase of the setup phase delay φ_S, due to the operation of an analog current modulator beyond its cutoff frequency.

3.4 Case study: SiGe thermoelectric microcooler

Thermoelectric coolers are able to achieve net subambient temperatures owing to the dominance of Peltier cooling over residual Joule heating. These physical mechanisms are known

Table 1: Overview of lock-in methods for frequency domain thermoreflectance imaging.

TECHNIQUE	PULSE / SIGNAL FREQUENCY				BANDWIDTH	COMPLEXITY
	DUT$^{(\star)}$	LED	Image	CCD	(order of magn.)	(# phase-locks)
HOMODYNE	$f/2$	0	f	$4f$	10 Hz	1
HETERODYNE 'four bucket' (Grauby *et al.* [7])	F	$2F+f$	f	$4f$	100 MHz	2
HETERODYNE 'cycled phase lag' (Vermeersch *et al.* [8])	F	$2F$	0	arbitrary	100 MHz	1

$^{(\star)}$ Assuming Joule effect; double DUT excitation freq. to capture Peltier effect at same thermal frequency.

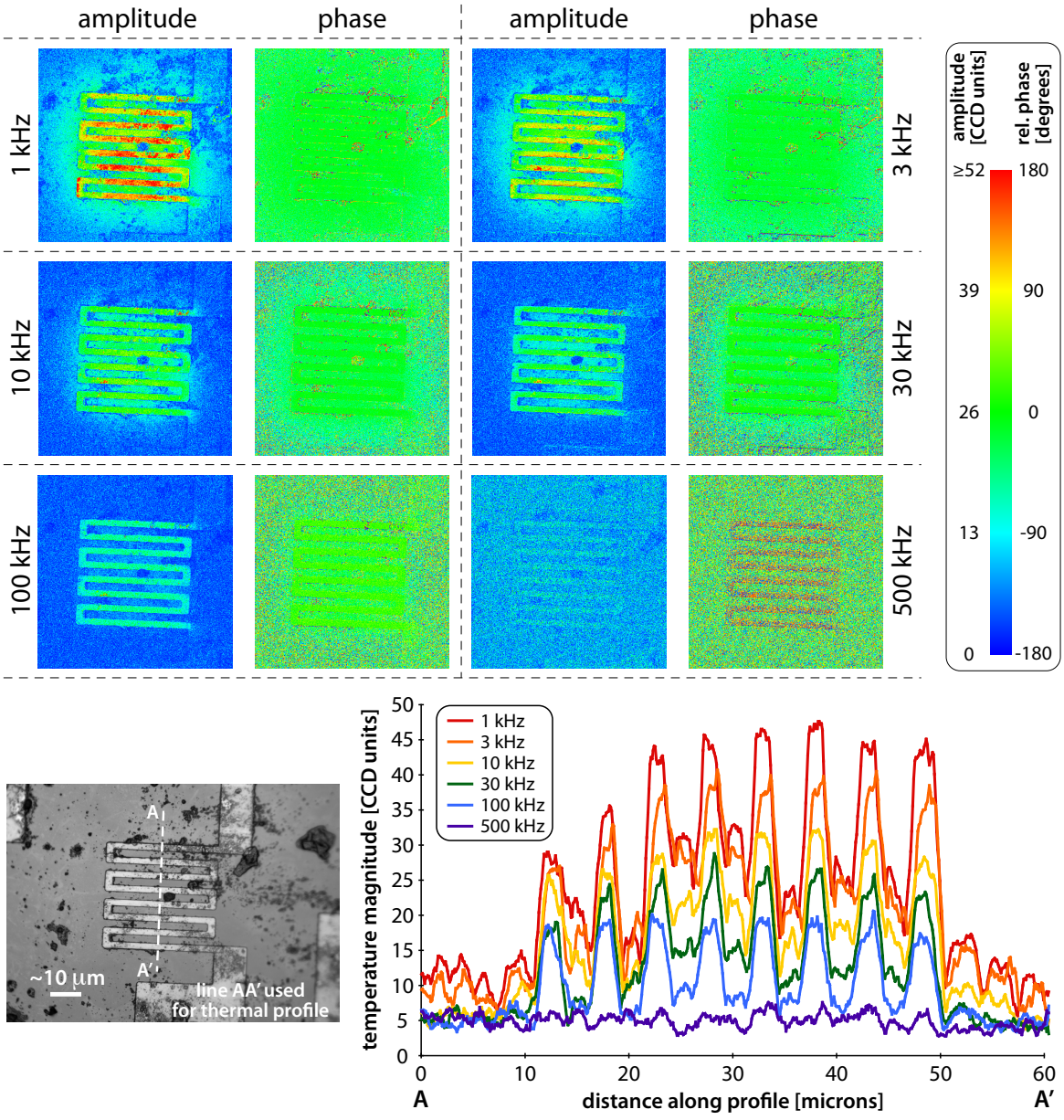

Figure 3: Frequency domain thermoreflectance imaging of a 40 micron heater using 'cycled phase lag' heterodyne lock-in (indicated frequencies are *thermal* frequencies).

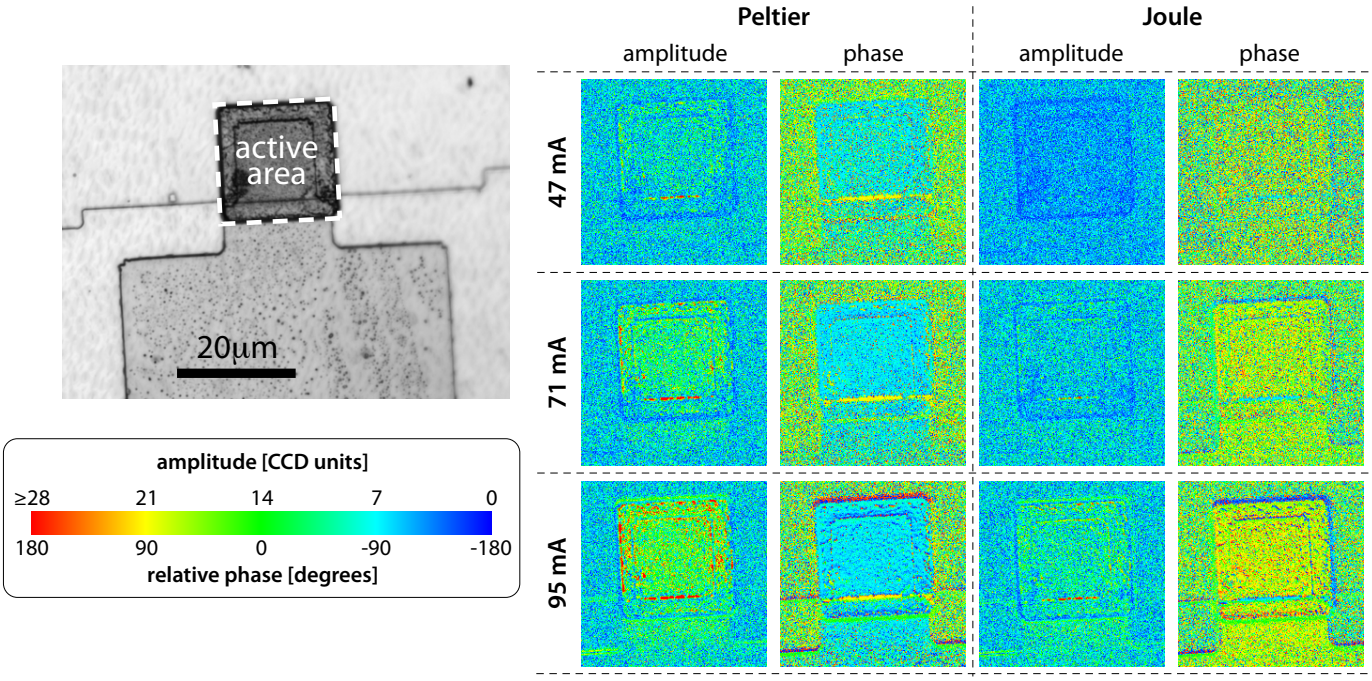

Figure 4: Frequency domain thermoreflectance imaging of a 20 micron thermoelectric cooler using 'cycled phase lag' heterodyne lock-in (indicated current excitations at 1 kHz).

to have a linear and quadratic dependence of the current bias, respectively. Hence, when exciting the cooler with a sinusoidal signal, the thermal effects will manifest themselves at different harmonics. Peltier and Joule effects can therefore be separated and studied completely independently using AC thermoreflectance, by simply locking into the right frequency. This feature is unique to frequency domain techniques, as transient measurements will always observe the superposition of the Peltier and Joule thermal signals.

We have analysed the behavior of a 20 micron SiGe superlattice cooler for various current biases. Figure 4 shows thermal images at the first (Peltier) and second (Joule) harmonics of the excitation. As we expect, the thermal signals become stronger when the current bias is increased. Overall the Joule component is clearly weaker than the Peltier term: the device is able to achieve net cooling in the considered current range. Further study has shown that the magnitude, averaged over the cooler's active area, varies almost linearly with the current bias in the Peltier case, while the Joule component shows more or less a parabolic tendency. We also notice a clear phase contrast between the two effects, with a difference that amounts systematically to about 180 degrees. This can be attributed to an opposite sign: Peltier cooling lowers the temperature while Joule heating increases it.

4. Conclusions

CCD-based thermoreflectance techniques enable quick, accurate and high-resolution thermal imaging of electronic devices. Both time domain and frequency domain approaches for transient characterisation were reviewed and compared. Pulsed boxcar averaging captures the entire transient heating curve of the device, as demonstrated for a microheater. We also presented a novel heterodyne lock-in technique that offers an easier implementation and enhanced accuracy compared to the tradional 'four bucket' technique adopted so far. Our method was used to image AC diffusion in an integrated heater, and to study Peltier and Joule effects separately in a thermoelectric microcooler.

Acknowledgements

B. Vermeersch developed a novel heterodyne thermoreflectance technique during his mandate as a Research Assistant for FWO - Vlaanderen and wishes to thank FWO for their Travel Grant sponsoring his exchange visit to UCSC.

References

1. M. Farzaneh, K. Maize, D. Lüerssen, J.A. Summers, P.M. Mayer, P.E. Raad, K.P. Pipe, A. Shakouri, R.J. Ram, J.A. Hudgings. CCD-based thermoreflectance microscopy: principles and applications. *Journal of Physics D: Applied Physics* **42**:Art. No. 143001, 2009.
2. P.M. Mayer, D. Lüerssen, R.J. Ram, J.A. Hudgings. Theoretical and experimental investigation of the thermal resolution and dynamic range of CCD-based thermoreflectance imaging. *Journal of the Optical Society of America A* **24**(4):1156–1163, 2007.
3. K. Maize, J. Christofferson, A. Shakouri. Transient thermal imaging using thermoreflectance. In *Proceedings of the 24th IEEE SEMI-THERM Symposium*, pp. 55–58, 2008.
4. J. Christofferson, Y. Ezzahri, K. Maize, A. Shakouri. Transient thermal imaging of pulsed-operation superlattice micro-refrigerators. In *Proceedings of the 25th IEEE SEMI-THERM Symposium*, pp. 45–49, 2009.
5. B. Vermeersch, G. De Mey. A shortcut to inverse Fourier

transforms: approximate reconstruction of the step response of distributed RC ladder networks from sparse frequency domain data. Submitted to *International Journal of Thermal Sciences* , 2009.

6. J. Altet, W. Claeys, S. Dilhaire, A. Rubio. Dynamic surface temperature measurements in ICs. *Proceedings of the IEEE* **94**(8):1519–1533, 2006.
7. S. Grauby, B.C. Forget, S. Holé, D. Fournier. High resolution photothermal imaging of high frequency phenomena using a visible charge coupled device camera associated with a multichannel lock-in scheme. *Review of Scientific Instruments* **70**(9):3603–3608, 1999.
8. B. Vermeersch, J. Christofferson, K. Maize, A. Shakouri. A novel heterodyne lock-in technique for CCD-based thermoreflectance imaging. To be submitted to *Journal of Physics D: Applied Physics* .